DØnote 4505, version 3.1

Flavor oscillations in B_d^0 mesons with same side tagging

The DØ Collaboration

(Dated: July 31, 2004)

$B_d^0 - \bar{B}_d^0$ oscillations were studied with a large semileptonic sample corresponding to approximately 250 pb^{-1} of integrated luminosity accumulated with the DØ Detector in Run II. The flavor of the final state of B_d^0 meson was determined using the muon charge from the partially reconstructed decay $B_d^0 \to \mu^+ D^*(2010)^- X$, $D^*(2010)^- \to \bar{D}^0 \pi^-$, $\bar{D}^0 \to K^+ \pi^-$. The same side tagging method was used for the initial-state flavor determination. The B_d^0 meson oscillation frequency and tagging purities for neutral and charged B-mesons were determined to be equal to:

$$\Delta m = 0.488 \pm 0.066\ (stat.) \pm 0.044\ (syst.)\ ps^{-1}$$
$$\eta_0 = 0.558 \pm 0.007\ (stat.) \pm 0.008\ (syst.)$$
$$\eta_+ = 0.622 \pm 0.008\ (stat.) \pm 0.012\ (syst.)$$

This benchmark result is an important step towards the B_s oscillation measurement.

I. INTRODUCTION

Measurements of flavor oscillations in B_d^0 mesons is an important topic in heavy flavor physics. The oscillations are explained in the Standard Model by box diagrams with top quarks and W bosons in the loop (Fig. 1). Those diagrams give rise to the difference between the two B_d^0 meson mass eigenstates, Δm. The precise measurement of the oscillation parameter Δm allows determination of the product of the CKM matrix elements $|V_{tb}V_{td}^*|^2$, see [1] for a recent overview of the subject.

The value of Δm has been measured with high precision at B-factories. The world average given in [2] is

$$\Delta m = 0.502 \pm 0.007 \text{ ps}^{-1} \tag{2}$$

The study of the $B_d^0 - \bar{B}_d^0$ mixing at the Tevatron is a benchmark measurement useful for understanding of the initial-state flavor tagging. Observation of oscillations in the B_s system is a major goal of the Tevatron physics program and there will be a lot of similarities between the flavor tagging for the B_s and B_d^0 mesons. It is also interesting because some theories predict "new physics" specific for hadron colliders (see for example [3]) which can affect the outcome of the mixing measurement for B_d^0 mesons at the Tevatron.

The analysis reported here exploits a large semileptonic sample corresponding to approximately 250 pb^{-1} of integrated luminosity, accumulated by DØ during the period from April 2002 to January 2004. B hadrons were selected using their semileptonic decays $B \to \mu^+ D^{*-} X$ (charge conjugated states are always implied in this paper) with reconstructed $D^{*-} \to \bar{D}^0 \pi^-$ decays. Both simulation and available experimental results show that this sample is dominated by $B_d^0 \to \mu^+ \nu D^{*-} X$ decays and can therefore be used to study oscillations of neutral B mesons.

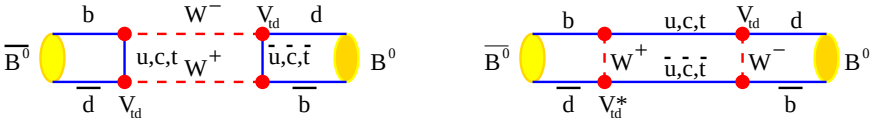

FIG. 1: Box diagrams responsible for $B_d^0 - \bar{B}_d^0$ oscillations.

II. DETECTOR DESCRIPTION

The following main elements of the DØ detector are essential for this analysis:

- A magnetic central-tracking system, which consists of a silicon microstrip tracker (SMT) and a central fiber tracker (CFT), both located within a 2 T superconducting solenoidal magnet;
- A muon system located beyond the calorimetry.

The SMT has $\approx 800,000$ individual strips, with typical pitch of $50 - 80$ μm, and a design optimized for tracking and vertexing capability at $|\eta| < 3$. The system has a six-barrel longitudinal structure, each with a set of four layers arranged axially around the beam pipe, and 16 radial disks. The CFT has eight thin coaxial barrels, each supporting two doublets of overlapping scintillating fibers of 0.835 mm diameter, one doublet being parallel to the collision axis, and the other alternating by $\pm 3^\circ$ relative to the axis. Light signals are transferred via clear light fibers to solid-state photon counters (VLPC) that have $\approx 80\%$ quantum efficiency.

The muon system consists of a layer of tracking detectors and scintillation trigger counters before 1.8 T toroids, followed by two additional layers after the toroids. Tracking at $|\eta| < 1$ relies on 10 cm wide drift tubes, while 1 cm mini-drift tubes are used at $1 < |\eta| < 2$.

III. DATA SAMPLE

This analysis uses the $B \to \mu^+ D^*(2010)^- X$ data sample selected with the offline filter from all data available before 1/21/2004 with no trigger requirement. In the offline filter muons were required to have transverse momentum $p_T^\mu > 2$ GeV/c as measured in the central tracker, pseudo-rapidity $|\eta^\mu| < 2$ and total momentum $p^\mu > 3$ GeV/c. All charged particles in a given event were clustered into jets using the DURHAM clustering algorithm [4]. Events with more than one identified muon in the same jet were rejected, as well as events with identified $J/\psi \to \mu^+\mu^-$ decays.

The $\bar{\mathrm{D}}^0$ candidate was constructed from two particles of the opposite charge belonging to the same jet as the reconstructed muon. Both particles are required to have transverse momentum $p_T > 0.7$ GeV/c, and pseudo-rapidity $|\eta| < 2$. They were required to form a common D-vertex with good fit χ^2. The vertexing algorithm is described in detail in [5]. For each particle, the axial (plane perpendicular to the beam direction) ϵ_T and stereo (plane parallel to the beam direction) ϵ_L projections of the track impact parameter with respect to the primary vertex together with the corresponding errors ($\sigma(\epsilon_T)$, $\sigma(\epsilon_L)$) were computed. The combined significance $\sqrt{(\epsilon_T/\sigma(\epsilon_T))^2 + (\epsilon_L/\sigma(\epsilon_L))^2}$ was required to be greater than 2. The distance d_T^D between the primary and D vertices in the axial plane was required to exceed 4 standard deviations: $d_T^D/\sigma(d_T^D) > 4$. The distance d_T^D was required to be less than 1.5 cm. The angle α_T^D between the $\bar{\mathrm{D}}^0$ momentum and the direction from the primary to the $\bar{\mathrm{D}}^0$ vertex in the axial plane was required to satisfy the condition: $\cos(\alpha_T^D) > 0.9$.

The tracks of muon and $\bar{\mathrm{D}}^0$ candidate were required to form a common B-vertex with good fit χ^2. The momentum of the B-candidate was computed as the sum of the momenta of the μ and $\bar{\mathrm{D}}^0$. The mass of the $(\mu^+\bar{\mathrm{D}}^0)$ system was required to fall within $2.3 < M(\mu^+\bar{\mathrm{D}}^0) < 5.2$ GeV/c^2. If the distance d_T^B between the primary and B vertices in the axial plane exceeded $4\sigma(d_T^B)$, the angle α_T^B between the B momentum and the direction from the primary to the B-vertex in the axial plane was demanded to satisfy the condition $\cos(\alpha_T^B) > 0.95$. The distance d_T^B was allowed to be greater than d_T^D, provided that the distance between the B and D vertices d_T^{BD} was less than $3\sigma(d_T^{BD})$. The decay length errors $\sigma(d_T^D)$ and $\sigma(d_T^B)$ were required to be less than 500 μm. The $Pt_{D^0} > 5$ GeV selection was used to make this analysis compatible with the semileptonic lifetime ratio analysis [6]. In total 433128 events passed these cuts (Fig.2).

The masses of kaon and pion were assigned to the particles according to the charge of the muon, requiring the $\mu^+K^+\pi^-$ final system or its charge conjugate. The invariant mass of $K\pi$ system for $\mu^+K^+\pi^-$ is shown in Fig.2. The curve shows the result of the fit of the $K^+\pi^-$ mass distribution with Gaussian and exponential background. The total number of D^0 candidates in the peak is 62070 ± 431. The left peak corresponds to partially reconstructed decay $\bar{D}^0 \to K^+\pi^- X$. Another Gaussian was used to fit its right slope.

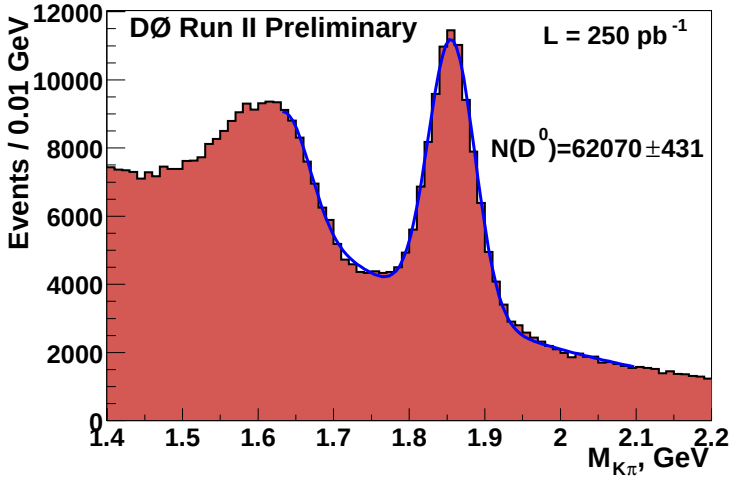

FIG. 2: The invariant mass of $K\pi$ system for $\mu^+K^+\pi^-$. The curve shows the result of the fit of the $K^+\pi^-$ mass distribution with Gaussian and exponential background. Total number of D^0 candidates in the peak is 62070 ± 431. The left peak corresponds to partially reconstructed decay $\bar{D}^0 \to K^+\pi^- X$. Another Gaussian was used to fit its right slope.

For the $\mu^+\bar{\mathrm{D}}^0$ candidates, we search for an additional pion (refered below as "slow pion") with $p_T > 0.18$ GeV/c and the charge opposite to the charge of the muon. The mass difference $\Delta M = M(\bar{\mathrm{D}}^0\pi) - M(\bar{\mathrm{D}}^0)$ for all such pions when $1.75 < M(\bar{\mathrm{D}}^0) < 1.95$ GeV/c^2 is shown in Fig. 3. The peak, corresponding to the production of $\mu^+\mathrm{D}^{*-}$ is clearly seen. The total number of D^{*-} candidates in the peak is equal to 17180 ± 164. In the fit function the signal and background have been approximated by a sum of two Gaussians and by a sum of an exponential and a linear function, respectively.

Below the $\mu^+D^{*\pm}$ candidates with mass difference $M_{K\pi\pi} - M_{K\pi} < 0.2$ GeV will be refered to as "D^* sample". The "D^* sample" consists of 62901 events which include both sign combinations for the slow pion. All other events belong to the "D^0 sample".

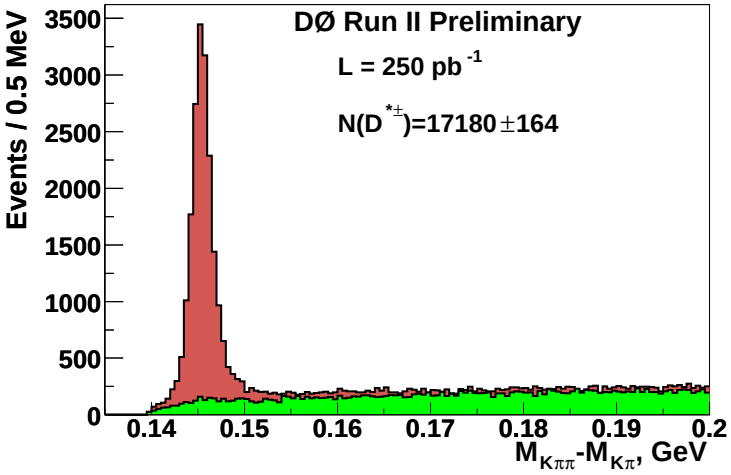

FIG. 3: The mass difference $M(\mathrm{D}^0\pi) - M(\mathrm{D}^0)$ for events with $1.75 < M(\mathrm{D}^0) < 1.95$ GeV/c^2. Total number of D* candidates is 17180 ± 164. In the fit function the signal and the background have been approximated by a sum of two Gaussians and by a sum of an exponential and a linear function, respectively.

IV. INITIAL STATE TAGGING WITH SAME SIDE TRACKS

The Same Side Tagging (SST) technique was first proposed by Gronau, Nippe and Rosner [7]. The technique has been used by several experiments to measure the B_d mixing [8, 9]. The main idea of the SST is that the charge of fragmentation pion correlates with the flavor of B-meson as illustrated in Figs. 4 and 5. A tagging algorithm needs to select the correct tagging track coming from the $\bar{b}$-quark fragmentation out of all tracks in some vicinity of the reconstructed B-meson. If the $\bar{b}$-quark fragmentation results in production of B^0 meson then the charged pion from fragmentation has sign "+" and correspondingly if a B^+ meson is produced the sign of the pion is "-". Thus the product of the muon and fragmentation pion charges in the case of semileptonic decays gives information about initial flavor of b-quark and its evolution in time. In the following this combination will be refered to as "correct sign combination" when the muon and fragmentation pion charges are the same for the D* sample and are opposite for the D^0 sample. The "wrong sign combination" will be refered to in the case when the muon and fragmentation pion charges are opposite for the D* sample and are the same for the D^0 sample.

To select the tagging track the algorithm considers all tracks in a cone of $dR < 0.7$ ($dR = \sqrt{(\Delta\phi)^2 + (\Delta\eta)^2}$) around the flight direction of B-meson. Here and below the parameters of B-meson are defined as parameters of the μD^0 system. All tracks have to come from the same primary vertex, have $Pt_{tag} > 0.5$ GeV, not to be associated with a muon and not to correspond to the reconstructed B-decay products. The number of SMT and CFT hits was required to be more than one for each detector. Some selections based on fragmentation theory were also applied to the tracks : total energy of tagging track and B meson, $E_{B\pi} > 12$ GeV; invariant mass of $B - \pi$ system, $M_{B\pi} < 5.5$ GeV; and transverse momentum of tagging track with respect to the B meson flight direction, $Pt_{rel} < 1$ GeV. It was assumed that the tag candidates are pions. On average, each B candidate had 2.04 tracks passing the above cuts.

The track with the lowest relative transverse momentum Pt_{rel} was taken as tag. The choice of the tagging variable was motivated by a good performance of this tagging algorithm for non-oscillating B$^+$ mesons and by the previous CDF experience in RunI analyses [8]. The distribution of Pt_{rel} for all tracks passing the above selections is shown in fig. 6.

The number of $\mu^+\bar{D}^0$ candidates in the D^0 sample before and after tagging was found to be equal to 38625 ± 336 and 28722 ± 307, respectively. The number of μ^+D^{*-} candidates in the D* sample before and after tagging was 17180 ± 164 and 12848 ± 146. The corresponding tagging efficiencies calculated from the above numbers are equal to $\epsilon_0 = 0.744 \pm 0.004$ for the D^0 sample and $\epsilon_* = 0.748 \pm 0.004$ for the D^* sample.

V. EXPERIMENTAL OBSERVABLES A_i

To describe the probability to change flavor over time one needs to define two observables which are measured experimentally : the flavor asymmetry and Visible Proper Decay Length (VPDL).

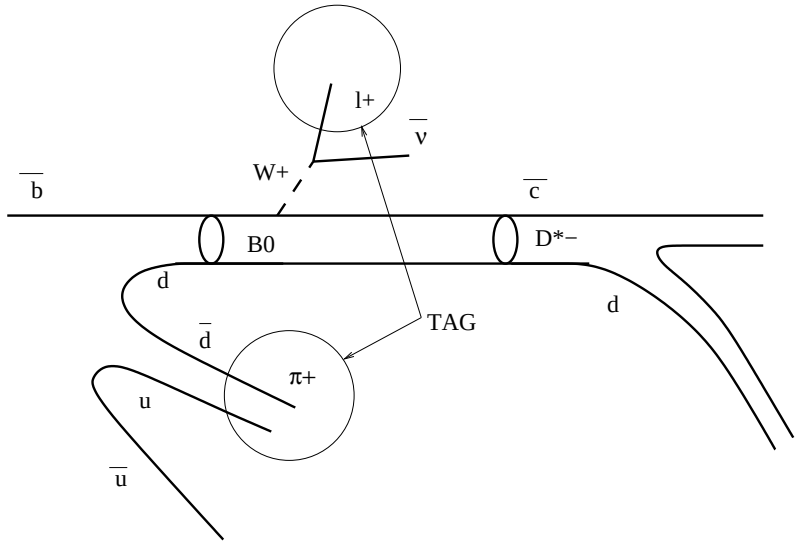

FIG. 4: SST schematic for B^0. $l^{\pm}\pi^{\pm}$ combinations give "correct sign combination" for B^0 meson.

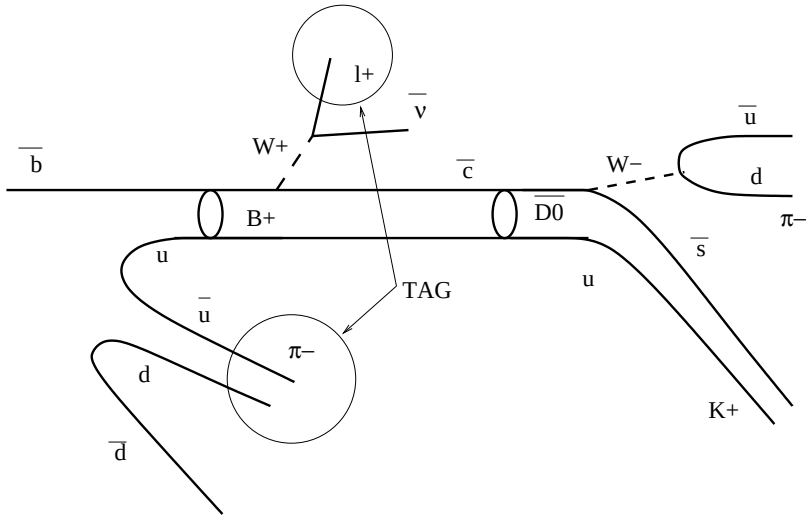

FIG. 5: SST schematic for B^+. $l^{\pm}\pi^{\mp}$ combinations give "correct sign combination" for $B^{\pm}$ meson.

The measured VPDL was calculated as $x^M = L_{xy} \cdot M_B \cdot c/P_T^{\mu \mathrm{D}^0}$ where the transverse decay length of a B-hadron L_{xy} was defined as the distance in the axial plane between the primary vertex and the vertex produced by the muon and $\bar{\mathrm{D}}^0$. The transverse momentum $P_T^{\mu \mathrm{D}^0}$ was defined as the vector sum of transverse momenta of muon and $\bar{\mathrm{D}}^0$. The sign of the decay length was set positive, if the angle α_T^B, defined in section III, was less than $\pi/2$, otherwise it was set negative.

Events were divided into 7 groups according to the measured VPDL. The number of $\mu^+\mathrm{D}^*$ events with "correct" and "wrong" tags, N_i^c and N_i^w, in each interval i of VPDL were determined from a fit of the D^* peak in the mass difference $M(\mathrm{D}^0\pi) - M(\mathrm{D}^0)$ distribution. The experimental observable, asymmetry A_i in each VPDL bin, for this measurement was defined as

$$A_i = \frac{N_i^c - N_i^w}{N_i^c + N_i^w} \tag{3}$$

for both $\mu^+\bar{D}^0$ and $\mu^+\mathrm{D}^{*-}$ samples.

Intervals of VPDL, the number of "correctly" and "wrongly" tagged events, the asymmetries and the corresponding errors derived from the fits in each VPDL bin are given in Tables I and II, respectively for the $\mu^+\bar{D}^0$ and $\mu^+\mathrm{D}^{*-}$ samples.

It is worth noting once again that the "correct" and "wrong" tags are always defined with respect to the re-

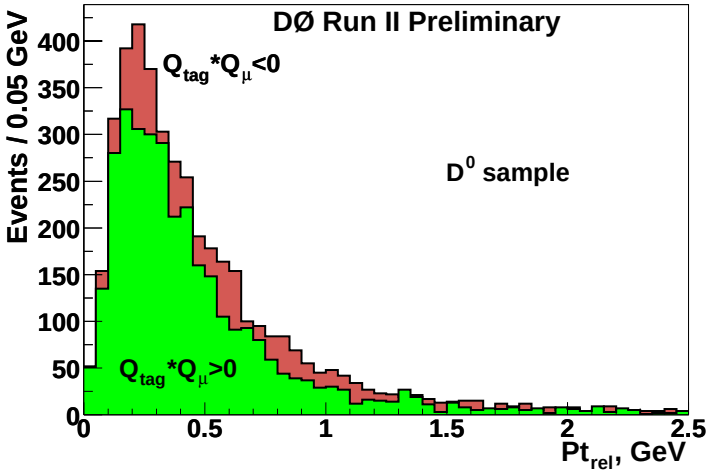

FIG. 6: D^0 sample. Distribution of the transverse momentum for the tagging track with respect to the B meson flight direction, Pt_{rel}.

TABLE I: D^0 sample. Definition of 7 intervals in VPDL. For each interval the measured number of D^0 candidates for the correct and wrong tag N_i^c, N_i^w, their statistical errors $\sigma(N_i^c)$, $\sigma(N_i^w)$, all determined from the fits of corresponding invariant mass $M(K\pi)$ distributions, the measured asymmetry A_i, its error $\sigma(A_i)$ and the expected asymmetry A_i^e corresponding to $\Delta m = 0.488$ ps^{-1} are given.

group	VPDL range, cm	$N_i^c \pm \sigma(N_i^c)$	$N_i^w \pm \sigma(N_i^w)$	$A_i \pm \sigma(A_i)$	A_i^e
1	$-0.025 \div 0.000$	933.99 ± 72.43	593.65 ± 58.35	0.223 ± 0.059	0.221
2	$0.000 \div 0.025$	4133.24 ± 129.15	2601.64 ± 105.77	0.227 ± 0.024	0.222
3	$0.025 \div 0.050$	3622.95 ± 109.73	2301.49 ± 90.49	0.223 ± 0.024	0.224
4	$0.050 \div 0.075$	2599.21 ± 94.83	1627.13 ± 87.86	0.230 ± 0.031	0.228
5	$0.075 \div 0.100$	1683.83 ± 81.48	1129.88 ± 57.75	0.197 ± 0.034	0.233
6	$0.100 \div 0.125$	1075.84 ± 60.09	715.17 ± 49.16	0.201 ± 0.042	0.238
7	$0.125 \div 0.250$	2182.40 ± 96.55	1191.86 ± 66.46	0.294 ± 0.033	0.249

constructed $\mu^+\bar{D}^0$ or $\mu^+\mathrm{D}^{*-}$ candidates according to the rules explained in IV. The asymmetry derived from the numbers of "correct" and "wrong" tags and its time evolution will depend on the purity of the tagging algorithm, sample composition and, of course, flavor oscillations as will be described in the next section.

VI. FITTING PROCEDURE

The following processes contribute to the D^* sample:

TABLE II: D^* sample. For each VPDL interval the measured number of D^* for the correct and wrong tag N_i^c, N_i^w, their statistical errors $\sigma(N_i^c)$, $\sigma(N_i^w)$, all determined from the fits of corresponding mass difference $M(\mathrm{D}^0\pi) - M(\mathrm{D}^0)$ distributions, the measured asymmetry A_i, its error $\sigma(A_i)$ and the expected asymmetry A_i^e corresponding to $\Delta m = 0.488$ ps^{-1} are given.

group	VPDL range, cm	$N_i^c \pm \sigma(N_i^c)$	$N_i^w \pm \sigma(N_i^w)$	$A_i \pm \sigma(A_i)$	A_i^e
1	$-0.025 \div 0.000$	448.028 ± 25.08	354.24 ± 23.27	0.117 ± 0.043	0.126
2	$0.000 \div 0.025$	1978.07 ± 48.28	1522.59 ± 44.03	0.130 ± 0.019	0.123
3	$0.025 \div 0.050$	1659.98 ± 43.57	1314.04 ± 39.90	0.116 ± 0.020	0.110
4	$0.050 \div 0.075$	1087.68 ± 35.19	959.67 ± 33.91	0.063 ± 0.024	0.087
5	$0.075 \div 0.100$	727.80 ± 28.70	634.71 ± 27.32	0.068 ± 0.029	0.058
6	$0.100 \div 0.125$	470.16 ± 23.37	461.62 ± 23.53	0.0092 ± 0.036	0.025
7	$0.125 \div 0.250$	774.72 ± 30.25	805.20 ± 30.99	-0.019 ± 0.027	-0.034

1. $B^0_d \to \mu^+\nu \mathrm{D}^{*-}$;
2. $B^0_d \to \mu^+\nu \mathrm{D}^{**-} \to \mu^+\nu \mathrm{D}^{*-}X$;
3. $B^+ \to \mu^+\nu \bar{\mathrm{D}}^{**0} \to \mu^+\nu \mathrm{D}^{*-}\pi^{**+}$.

and to the D^0 sample:

4. $B^+ \to \mu^+\nu \bar{\mathrm{D}}^0$;
5. $B^+ \to \mu^+\nu \bar{\mathrm{D}}^{*0} \to \mu^+\nu \bar{\mathrm{D}}^0$;
6. $B^+ \to \mu^+\nu \bar{\mathrm{D}}^{**0} \to \mu^+\nu \bar{\mathrm{D}}^0 X$;
7. $B^+ \to \mu^+\nu \bar{\mathrm{D}}^{**0} \to \mu^+\nu \bar{\mathrm{D}}^{*0} X \to \mu^+\nu \bar{\mathrm{D}}^0 X$;
8. $B^0_d \to \mu^+\nu \mathrm{D}^{**-} \to \mu^+\nu \bar{\mathrm{D}}^0 \pi^{**-}$;
9. $B^0_d \to \mu^+\nu \mathrm{D}^{**-} \to \mu^+\nu \bar{\mathrm{D}}^{*0} \pi^{**-} \to \mu^+\nu \bar{\mathrm{D}}^0 \pi^{**-} X$;
10. $B^0_d \to \mu^+\nu \mathrm{D}^{*-}$ (with lost π_*);
11. $B^0_d \to \mu^+\nu \mathrm{D}^{**-} \to \mu^+\nu \mathrm{D}^{*-} X$ (with lost π_*).

Note that both D^0 and D^* samples have contributions from B^+ and B_d mesons. As will be shown in the following the D^* sample is composed mostly of B^0_d mesons with some contributions from B^+ mesons and oppositely the D^0 sample is composed mostly of B^+ mesons with some contributions from B^0_d mesons. Possible contributions from B_s mesons and b-baryons to the sample are small and were neglected for this analysis.

Because D^{**} mesons are not reconstructed in this analysis the track produced by the charged pion from D^{**} decay, π^{**}, can be taken as a tag track in processes 3, 8, 9 as illustrated in fig. 7, 8. If correct fragmentation pion is taken as a tag track then it gives wrong sign combination with muon from B-decay (compare fig. 7 with fig. 5 and fig. 8 with fig. 4). If the π^{**} track is reconstructed then there is a probability that this track will be taken as a tag. In this case the correlation between signs of this track and muon from B-decay will be always correct for both B^+ and B^0 cases and, therefore, these three processes will need a special treatment in the fitting procedure. Here and in the following the symbol "D^{**}" denotes both narrow and wide D^{**} resonances, together with non-resonant $\mathrm{D}\pi$ and $\mathrm{D}^*\pi$ production and it is assumed that D^{**} decays are saturated by the single pion modes.

The distributions of VPDL for different processes in the D^0 and D^* samples are listed below taking into account that different species of B-mesons behave differently with respect to oscillations. Neutral B^0_d mesons do oscillate while charged B^+ mesons do not oscillate. The purity of the tagging method was defined as $\eta = N_{correctly\ tagged\ events}/N_{total\ tagged\ events}$. Note that it relates to the commonly used definition of dilution as $\mathcal{D} = (N_{correctly\ tagged\ events} - N_{wrongly\ tagged\ events})/N_{total\ tagged\ events} = 2\eta - 1$. The purities for B^0 and B^+, η_0 and η_+, are different due to differences in fragmentation of charged and neutral B-mesons.

Processes contributing to the D^* sample:

- $B^0_d \to \mu^+\nu \mathrm{D}^{*-}$ and $B^0_d \to \mu^+\nu \mathrm{D}^{**-} \to \mu^+\nu \mathrm{D}^{*-}X$:

$$n^c_{j=1,2}(x) = \frac{K}{c\tau_{B^0}} \exp(-\frac{Kx}{c\tau_{B^0}}) \cdot 0.5 \cdot (1 + (2\eta_0 - 1)\cos(\Delta m \cdot Kx/c)) \tag{4}$$

$$n^w_{j=1,2}(x) = \frac{K}{c\tau_{B^0}} \exp(-\frac{Kx}{c\tau_{B^0}}) \cdot 0.5 \cdot (1 - (2\eta_0 - 1)\cos(\Delta m \cdot Kx/c)) \tag{5}$$

  where $K = P_T^{\mu \mathrm{D}^0}/P_T^B$ here and below is a K-factor reflecting the difference between the observed and true momentum of the B-hadron, τ_B is the lifetime of B-hadrons [2] and x is the expected VPDL. Subscript j corresponds to different decay channels as defined in the beginning of the section.

- $B^+ \to \mu^+\nu \bar{\mathrm{D}}^{**0} \to \mu^+\nu \mathrm{D}^{*-}\pi^{**+}X$. In this case we need to divide events into two parts: one when π^{**} was taken as a tag - marked as "**" - and all other events. The "**" part will have only events with "correct" sign combination. Parameter P^{**} describes the probability for π^{**} to be taken as a tag track in this process.

$$n^c_{j=3**}(x) = P^{**} \cdot \frac{K}{c\tau_{B^+}} \exp(-\frac{Kx}{c\tau_{B^+}}) \tag{6}$$

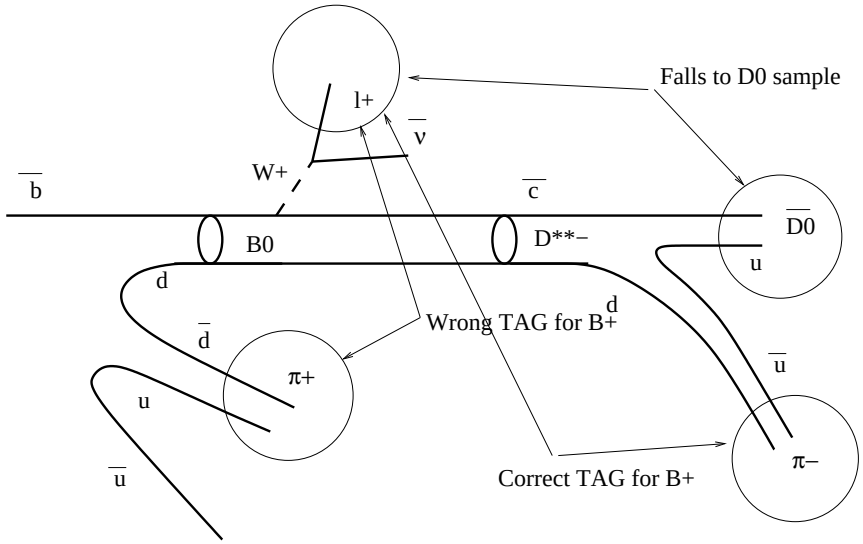

FIG. 7: Schematic diagram of SST for B^0 decaying to D^{**}.

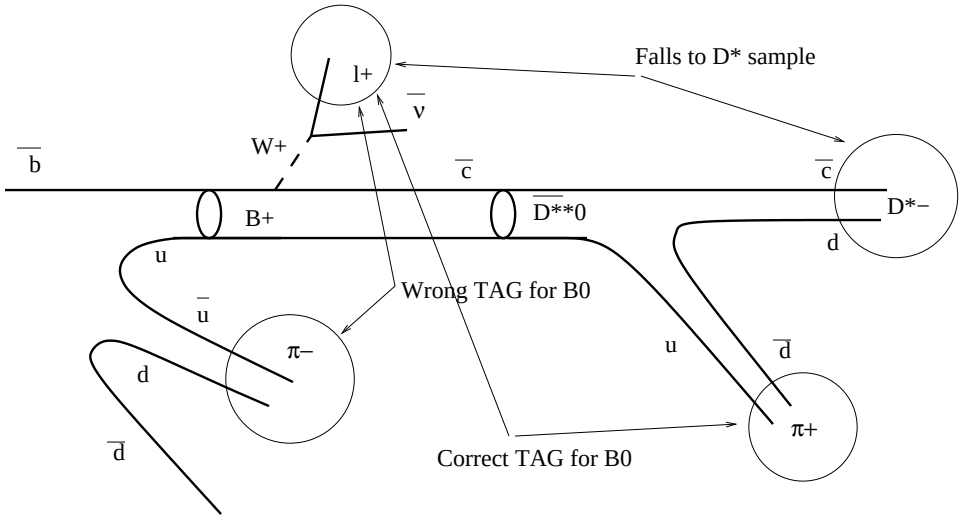

FIG. 8: Schematic diagram of SST for B^+ decaying to D^{**}.

$$n^c_{j=3}(x) = \frac{K}{c\tau_{B^+}} \exp(-\frac{Kx}{c\tau_{B^+}}) \cdot (1-\eta_+) \tag{7}$$

$$n^w_{j=3}(x) = \frac{K}{c\tau_{B^+}} \exp(-\frac{Kx}{c\tau_{B^+}}) \cdot \eta_+ \tag{8}$$

Processes contributing to the D^0 sample:

- The first four processes in the D^0 sample:

$$n^c_{j=4-7}(x) = \frac{K}{c\tau_{B^+}} \exp(-\frac{Kx}{c\tau_{B^+}}) \cdot \eta_+ \tag{9}$$

$$n^w_{j=4-7}(x) = \frac{K}{c\tau_{B^+}} \exp(-\frac{Kx}{c\tau_{B^+}}) \cdot (1-\eta_+) \tag{10}$$

- The processes $B_d^0 \to \mu^+\nu \mathrm{D}^{**-} \to \mu^+\nu\bar{\mathrm{D}}^0\pi^{**-}$ and $B_d^0 \to \mu^+\nu \mathrm{D}^{**-} \to \mu^+\nu\bar{\mathrm{D}}^{*0}\pi^{**-} \to \mu^+\nu\bar{\mathrm{D}}^0\pi^{**-}X$ also need to be divided into two parts: one when π^{**} was taken as a tag and all other events.

$$n^c_{j=8**,9**}(x) = P^{**} \cdot \frac{K}{c\tau_{B^0}} \exp(-\frac{Kx}{c\tau_{B^0}}) \tag{11}$$

$$n^c_{j=8,9}(x) = \frac{K}{c\tau_{B^0}} \exp(-\frac{Kx}{c\tau_{B^0}}) \cdot 0.5 \cdot (1 - (2\eta_0 - 1)\cos(\Delta m \cdot Kx/c)) \tag{12}$$

$$n^w_{j=8,9}(x) = \frac{K}{c\tau_{B^0}} \exp(-\frac{Kx}{c\tau_{B^0}}) \cdot 0.5 \cdot (1 + (2\eta_0 - 1)\cos(\Delta m \cdot Kx/c)) \tag{13}$$

- The processes $B_d^0 \to \mu^+\nu \mathrm{D}^{*-}$ and $B_d^0 \to \mu^+\nu \mathrm{D}^{**-} \to \mu^+\nu \mathrm{D}^{*-}X$ (both with lost π_*) :

$$n^c_{j=10,11}(x) = \frac{K}{c\tau_{B^0}} \exp(-\frac{Kx}{c\tau_{B^0}}) \cdot 0.5 \cdot (1 - (2\eta_0 - 1)\cos(\Delta m \cdot Kx/c)) \tag{14}$$

$$n^w_{j=10,11}(x) = \frac{K}{c\tau_{B^0}} \exp(-\frac{Kx}{c\tau_{B^0}}) \cdot 0.5 \cdot (1 + (2\eta_0 - 1)\cos(\Delta m \cdot Kx/c)) \tag{15}$$

The K-factors were determined from the simulation using generator-level information for the computation of p_T^B and $P_T^{\mu\mathrm{D}^0}$. The slow pion from D^{*-}decay was not included in the $p_T(\mu\mathrm{D}^0)$ computation for the K-factors. The K-factors for all considered decays were combined into four groups: $B \to \mu^+\nu\bar{\mathrm{D}}^0X$. $B \to \mu^+\nu\bar{\mathrm{D}}^*X$, $B \to \mu^+\nu\bar{\mathrm{D}}^{**}X \to \mu^+\nu\bar{\mathrm{D}}^0X$, $B \to \mu^+\nu\bar{\mathrm{D}}^{**}X \to \mu^+\nu\bar{\mathrm{D}}^*X$,

Transition to the measured VPDL, x^M, is achieved by integration over K-factors and resolution functions:

$$N_j^{c,\ w}(x^M) = \int dx\ Res_j(x - x^M) \cdot Eff_j(x) \int dK\ D_j(K) \cdot \theta(x) \cdot n_j^{c,\ w}(x, K). \tag{16}$$

Here $Res_j(x - x^M)$ is the detector resolution of the VPDL and $Eff_j(x)$ is the reconstruction efficiency for a given decay channel j of this type of B meson. The step function $\theta(x)$ takes into account that only positive values of x are possible (x^M can have negative values due to resolution effects). The function $D_j(K)$ gives the normalized distribution of the K-factor in a given channel j.

The resolution and efficiency are both determined from the simulation. In this case the simulation includes the detailed GEANT description of the detector and the full reconstruction chain. The decay length resolution was parameterised by the sum of 3 Gaussians with the following parameters: widths 26, 56 and 141 microns; relative normalizations 0.423, 0.505 and 0.072 respectively. Since the slow pion is not used in the B-vertex the resolution should be the same for the D^0 and D^* samples. This assumption has been confirmed both in MC and in the data. The efficiency to reconstruct the slow pion was found to be equal to 88%.

The expected number of events with "correct, wrong" tags in the i-th bin of VPDL is equal to

$$N_i^{e;c,w} = \int_i dx^M \ \sum_j (Br_j \cdot N_j^{c,w}(x^M)) \tag{17}$$

Here the integration $\int_i dx^M$ is taken over a given interval i, the sum $\sum_j$ is taken over all contributing decay channels and Br_j is the branching ratio of a given channel j.

The latest PDG values [2] were used for the B decay branching fractions. Exploiting the fact that semileptonic B decays are saturated by decays to D, D^* and D^{**} , and the isotopical invariance it was determined that the B_d^0 (88%) and B^+ (12%) decays give the main contributions into the D^* sample. The corresponding contributions to the D^0 sample are 16% and 84%. The above numbers include the reconstruction efficiencies for all contributing channels.

Finally, the expected asymmetry A_i^e for interval i of the measured VPDL is given by formula (3) with N_i^c and N_i^w substituted by $N_i^{e,c}$ and $N_i^{e,w}$.

The fit values of Δm, η_0 and η_+ were determined from the minimization of a $\chi^2(\Delta m, \eta_0, \eta_+)$ defined as:

$$\chi^2(\Delta m, \eta) = \sum_i \frac{(A_i - A_i^e(\Delta m, \eta_0, \eta_+))^2}{\sigma^2(A_i)} \tag{18}$$

The variables $\Delta m,\ \eta_0,\ \eta_+$ were the only free parameters of the fit.

VII. D^{**} TOPOLOGICAL ANALYSIS

Topology of the event has been used to measure the probability of pions from D** decays, π^{**}, to be selected as tagging track. This probability is used to determine the contribution of those cases to the expected asymmetry. Despite the contribution may not be large it plays an important role because of the 100% correlation of the π^{**} charge and the flavor of the decaying B-meson (i.e. effectively 100% purity and dilution for this kind of events).

The tagging track which originated from the primary vertex has wide distribution of the impact parameter significances with respect to the secondary B-vertex (IPSB). On the contrary the IPSB of the π^{**} has a narrow distribution because this track belongs to this vertex. The tagged events with the "wrong" sign combination never have a π^{**} track taken as tag. Therefore, using these events one can determine the shape of the IPSB distribution for the tracks originated in the primary vertex. Then this shape can be used together with a narrow Gaussian describing the contribution from π^{**}'s to fit the correct sign combination. The distribution of impact parameter significance for tagging tracks with respect to the B-vertex in the xy plane is shown in Fig.9 for the D^0 sample. Excess of events with low IPSB is interpreted as contribution from the D**channels. Additional tighter cuts, on the decay length significance, $L_{xy}/\sigma_{L_{xy}} > 3$, and on the D^0 mass window: $1.8 < M_{K\pi} < 1.92$ GeV, were applied to obtain these distributions for the D^0 sample:

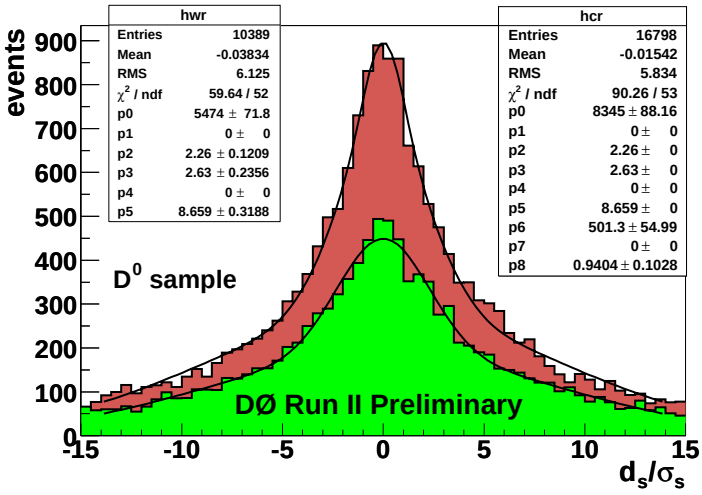

FIG. 9: Distribution of the impact parameter significance for tagging tracks with respect to the B-vertex in the xy plane for the D^0 sample.

The fit gives the number of D^{**} for the D^0 sample $N_0^{**} = 1003 \pm 110$ which corresponds to the probability to take π^{**} as a tag track in that sample of $R_0^{**} = 4.7 \pm 0.5\%$.

The probability P^{**} to take π^{**} as a tag in the processes $B_d^0 \to \mu^+ \nu \mathrm{D}^{**-} \to \mu^+ \nu \bar{\mathrm{D}}^0 \pi^{**-} X$ was determined as:

$$P^{**} = R_0^{**} \cdot \epsilon_0 / F_{D_0^{**}} = 0.255, \tag{19}$$

where $F_{D_0^{**}} = 13.6\%$ is relative contribution of channels with D** into the D^0 sample derived from the known sample composition. P^{**} is used in all equations containing the "**" symbol in the previous section to estimate contributions from the D** processes. Here and above it was assumed that the parameter P^{**} is the same for the D^0 and D* samples. This assumption is supported by the fact that a dominant fraction of D** decays to D^0 through intermediate D^{*0} (see [2]) which should result in similar kinematics of these processes.

VIII. RESULTS

The result of the minimization is:

$$\begin{aligned} \Delta m &= 0.488 \pm 0.066 \ (stat.) \ ps^{-1} \\ \eta_0 &= 0.558 \pm 0.007 \\ \eta_+ &= 0.622 \pm 0.008 \end{aligned} \tag{20}$$

The obtained values of A_i^e in each bin are given in the last column of Tables I and II. The value of χ^2/NDF in the minimum is 5.9/11.

Figure 10 show the asymmetries as functions of VPDL together with the result of the fit. Due to the contribution from B^0 events the fit function raises with VPDL for the D^0 sample. The contribution of B^+ events into the D^* sample results in the positive offset shift of the asymmetry.

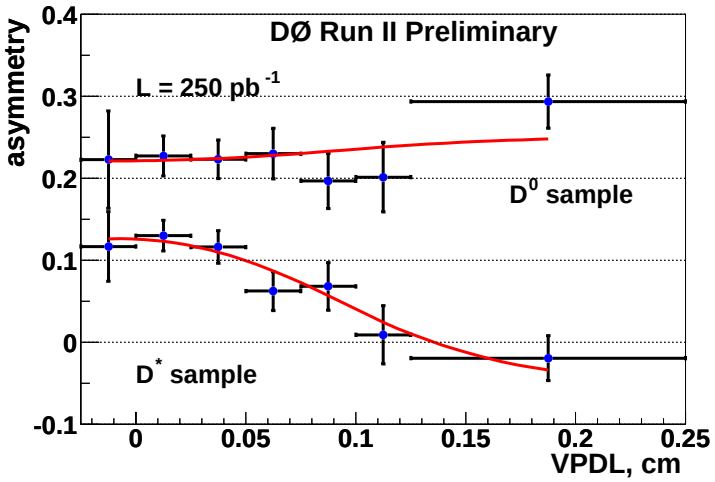

FIG. 10: Asymmetry as function of VPDL together with result of the combined fit for the D^0 and D^* samples.

IX. SYSTEMATIC ERRORS

A summary of the systematic errors is given in Table III. It shows variations of Δm, η_0 and η_+ for each considered systematic effect. Only the most important contributions are shown in the table.

TABLE III: Systematic errors and cross checks

	variation	Δm change, ps^{-1}	η_0 change	η_+ change
Bs contribution	all Bs modes included	0.008	0.003	0.002
$Br(B^0 \to D^{*-}\mu^+\nu)$	$5.53 \pm 0.23\%$	0.003	0.001	0.001
$Br(B^\pm \to D^*\pi\mu\nu X)$	$1.07 \pm 0.25\%$	0.017	0.001	0.001
$\Delta\tau/\tau$	0.086 ± 0.017	0.001	0.001	0.001
resolution	x[$1 \div 2$]	0.005	0.001	0.000
alignment	10μm	0.007	0.004	0.004
k-factor	average value $\pm$ 2%	0.009	0.000	0.004
MC efficiency	all equal to 100%	0.008	0.001	0.010
D** contribution	$R_0^{**} = 4.7 \pm 0.6\%$	0.035	0.004	0.004
$c\bar{c}$	see text	0.001	0.002	0.001
D^0 fitting procedure	see text	0.005	0.001	0.003
D^* fitting procedure	see text	0.007	0.002	0.000
binning in D^0 sample	from 80 to 160	0.003	0.000	0.000
binning in D^* sample	from 130 to 200	0.001	0.000	0.000
Total systematic error		0.044	0.008	0.012

The branching rates of B mesons used as input for minimization were varied by 1σ. The charged and neutral B meson lifetime ratio was varied by one σ to estimate the corresponding contribution to the systematic error.

The VPDL resolution, obtained from the simulation, was varied by a large factor, from 1 to 2, which significantly exceeds the estimated difference in resolution between data and simulation.

Variation of K-factors with B momentum was neglected in this analysis. To check the impact of this assumption on the final result, their computation was repeated without a cut on $p_T(\mathrm{D}^0) > 5$ GeV/c, or by applying an additional

cut at 4 GeV/c on p_T of muon. The change of average value of K-factors did not exceed 2%, which was used as the estimate of the systematic uncertainty in their values.

The systematic error from incorrect modelling of the MC efficiency was estimated assuming equal (100%) efficiencies for all contributing processes.

One of the most important systematic uncertainties arises from the determination of probability to use π^{**} as tag track, mostly due to the statistical incertainty in determination of $R_0^{**} = 4.7 \pm 0.5\%$. Precision of this parameter is limited by statistics in the available D^0 sample used for its evaluation (see Sec. VII). A possible R_0^{**} systematic bias was also considered as described below.

It is known [2] that in addition to the decays $D^{**} \to D^{0/*-}\pi^+$ there exist also decays $D^{**} \to D^{0/*-}\pi^+\pi^-$. These type of events results in an additional track coming from the B vertex even for the events with wrong tag. A possible bias from the double pion decay modes was estimated in the data exploiting the event topology and as a result the error on R_0^{**} has been increased from 0.5% to 0.6%. The 0.6% error on R_0^{**} is translated to the Δm systematic error of 0.035 ps^{-1}.

$c\bar{c}$ events originating from gluon splitting can mimic the signature $\mu^- D^{*+}$ when one c-quark decays semileptonically and the other fragments into D^*. Since μ and D^* come from different charm quarks one can expect that the quasi B vertices built by the muon and D^0 track will be concentrated in the vicinity of the primary vertex. There are experimental indications that the $c\bar{c}$ contribution if present affects only two first VPDL bins and for the preliminary evaluation of the corresponding systematic error the first two VPDL bins have been excluded from the minimisation procedure. The determined difference in the result was taken as the corresponding systematic error.

Different fitting functions were used to evaluate the systematic error from mass peak fitting procedure. For the D^0 sample the fitting function was changed to *Gaussian+Linear*. For the D^* sample the number of signal events was calculated as a difference in number of events in the correct sign histogram and background function in the mass window $0.14 < M_{K\pi\pi} - M_{K\pi} < 0.15 GeV$. In both cases the difference in Δm was taken as corresponding systematics error.

The mass peak and asymmetry fitting procedures have been also validated by toy MC experiments.

X. CONCLUSIONS

We reported a preliminary measurement of the B_d^0 meson oscillation frequency. The large semileptonic sample corresponding to approximately 250 pb^{-1} of integrated luminosity, accumulated by DØ during period from April 2002 to January 2004, was analysed and more than 17000 ($\mu^+ \mathrm{D}^{*-} X$) candidate events were selected for the analysis. The same side tagging method was used for the initial-state flavor determination. Using these statistics, the B_d^0 meson oscillation frequency and tagging purities for neatral and charged B-mesons were determined to be equal to:

$$\begin{aligned} \Delta m &= 0.488 \pm 0.066\ (stat.) \pm 0.044\ (syst.)\ ps^{-1} \\ \eta_0 &= 0.558 \pm 0.007\ (stat.) \pm 0.008\ (syst.) \\ \eta_+ &= 0.622 \pm 0.008\ (stat.) \pm 0.012\ (syst.) \end{aligned} \tag{21}$$

This result is in agreement with the world average of $\Delta m = 0.502 \pm 0.007\ \mathrm{ps}^{-1}$.

Acknowledgments

We thank the staffs at Fermilab and collaborating institutions, and acknowledge support from the Department of Energy and National Science Foundation (USA), Commissariat à l'Energie Atomique and CNRS/Institut National de Physique Nucléaire et de Physique des Particules (France), Ministry of Education and Science, Agency for Atomic Energy and RF President Grants Program (Russia), CAPES, CNPq, FAPERJ, FAPESP and FUNDUNESP (Brazil), Departments of Atomic Energy and Science and Technology (India), Colciencias (Colombia), CONACyT (Mexico), KRF (Korea), CONICET and UBACyT (Argentina), The Foundation for Fundamental Research on Matter (The Netherlands), PPARC (United Kingdom), Ministry of Education (Czech Republic), Natural Sciences and Engineering Research Council and WestGrid Project (Canada), BMBF (Germany), A.P. Sloan Foundation, Civilian Research and Development Foundation, Research Corporation, Texas Advanced Research Program, and the Alexander von Humboldt Foundation.

[1] Z.Ligetti "Introduction to heavy meson decays and CP asymmetries", hep-ph/0302031

[2] K. Hagiwara *et al.*, Phys. Rev. **D66**, 010001 (2002) and 2003 off-year partial update for the 2004 edition available on the PDG WWW pages (URL: http://pdg.lbl.gov/)
[3] E.Berger *et al.,* Phys. Rev. Lett. **86**, 4231 (2001).
[4] S.Catani *et al.*, Phys. Lett. **B269** (1991) 432.
[5] DELPHI Collab., *b-tagging in DELPHI at LEP*, Eur. Phys. J. **C32** (2004), 185-208
[6] J.Stark, B Physics at DZero, hep-ex/0407002.
[7] M. Gronau *et al.*, Phys. Rev. D 49, (1994), 254.
[8] CDF SST analyses
[9] LEP SST analyses
[10] P. Maksimovic, PhD. Thesis "Observation of $\pi - B$ meson Charge-Flavor Correlations and Measurement of Time Dependent $B^0\bar{B}^0$ Mixing in $p\bar{p}$ Collisions" (1998)